Supporting Material of the manuscript:

Towards optimal design of cancer nanomedicines: Multi-stage nanoparticles for the treatment of solid tumors

T. Stylianopoulos, E. A. Economides, J. W. Baish, D. Fukumura, R. K. Jain

Description of the Mathematical Model

We represent the tumor vasculature as a 2-dimensional percolation network at the percolation threshold, with one inlet and one outlet as shown in Supplementary Fig. 1 [1]. These network structures have been found to represent tumor vasculature in animal models well [10], though real angiography images could be used to represent additional heterogeneity present in unusual vascular networks or be applied to 3-dimensional structures. We repeated the simulations for five network realizations and the average values are presented.

Fluid Flow Equations

The mathematical model requires coupling of fluid flow in the vascular and interstitial spaces. Blood flow rate in a vessel ($Q_{vascular}$) is assumed to be axial and follows Poiseuille's equation [18],

$$Q_{vascular} = -\frac{\pi d^4}{128\mu}\frac{\Delta p_V}{\Delta x}, \tag{1}$$

where d is the vessel diameter, Δp_v is the vascular pressure difference that corresponds to a vascular length Δx and μ is the blood viscosity.

Fluid flow rate across the vessel wall ($Q_{transvascular}$) follows Starling's approximation [3],

$$Q_{transvascular} = L_p S\left(p_V - p_i\right), \tag{2}$$

where L_p is the hydraulic conductivity of the vessel wall, S is the surface area of the vessel and p_i is the interstitial fluid pressure. In the equation above, we neglect osmotic pressures.

Interstitial volumetric fluid flow rate (Q_{tissue}) follows Darcy's law,

$$Q_{tissue} = -K_t A_C \frac{\Delta p_i}{\Delta x}, \tag{3}$$

where K_t is the hydraulic conductivity of the interstitial space and Δp_i is the interstitial pressure difference that corresponds to a tissue length Δx. Δx is the distance between two interstitial nodes (Supplementary Fig. 1 B), taken to be 50 μm, the same as the vascular length in Eq. 1. A_c is the tissue cross-sectional area, which is related to the vascular density, S_v, and the diameter of the vessel, d, by $A_C = \pi d / S_V$ (Ref. [2]).

Drug Delivery Equations

Coupling of nanoparticle transport between the vascular and interstitial spaces is based on the following assumptions.

Inside the blood vessels diffusion is negligible and thus, the mass balance is convection dominated:

$$\frac{dc_V}{dt} = -u\frac{\Delta C_V}{\Delta x}, \tag{4}$$

where u is the axial blood velocity which is determined by dividing $Q_{vascular}$ in Eq. 1 by the cross sectional area of the vessel, C_v is the intravascular concentration of the nanoparticle and ΔC_v is the concentration difference that corresponds to a vascular length Δx.

The amount Φ of nanoparticles (or drug for a single stage system) that is transferred across the vessel wall between the vascular and interstitial space is given by Starling's approximation as [3]

$$\Phi = L_p S(p_V - p_i)(1-\sigma)\frac{C_V e^{Pe} - c_i}{e^{Pe}-1} \quad \text{with} \quad Pe = L_p(1-\sigma)\frac{\left(p_V - p_i\right)}{P}, \tag{5, 6}$$

where Pe is the Péclet number across the vessel wall, and P is the vascular permeability of the nanoparticle through the pores of the wall. Therefore, Φ is subtracted from Eq. 4 and added to the equation for the interstitial transport of the nanoparticles, as shown in Eqns. 12, 15 and 19 for the three delivery systems.

Using theory for transport of particles through cylindrical pores we calculate the hydraulic conductivity, L_p, vascular permeability, P, and reflection coefficient, σ, by the equations [6]:

$$L_p = \frac{\gamma r_o^2}{8\mu L},\ P = \frac{\gamma H D_O}{L},\ \sigma = 1 - W, \tag{7}$$

where γ is the fraction of vessel wall surface area occupied by pores, r_o is the pore radius, L is the thickness of the vessel wall, and D_o is the diffusion coefficient of the particle in free solution at 37 ^{o}C.

The parameters H and W account for hydrodynamic and electrostatic interactions and for dilute solutions are given by the equations [6]:

$$H = 2\int_0^{1-\lambda} K^{-1} e^{-E/kT}\beta d\beta, \tag{8}$$

$$W = 4\int_0^{1-\lambda} G\left(1-\beta^2\right)e^{-E/kT}\beta d\beta, \tag{9}$$

where λ is the ratio of the particle size over the pore size, E is the electrostatic energy of interaction between the nanoparticle and the pore, k is Boltzmann's constant, T is the absolute temperature, $K(\lambda,\beta)$ and $G(\lambda,\beta)$ are hydrodynamic functions, and β is the

radial distance of the particle inside the pore divided by the pore radius to become dimensionless.

To calculate the hydrodynamic functions, *K(λ,β)* and *G(λ,β)*, the centerline approximation is employed, which suggests that use of the centerline values, *K(λ,0)* and *G(λ,0)* leads to reasonably accurate estimates of *H* and *W*. Therefore, Eqs 8-9 are written as:

$$H = 2K^{-1}(\lambda,0)\int_0^{1-\lambda} e^{-E/kT}\beta d\beta \quad , \tag{10}$$

$$W = 4G(\lambda,0)\int_0^{1-\lambda}\left(1-\beta^2\right)e^{-E/kT}\beta d\beta \quad . \tag{11}$$

Analytical expressions of the hydrodynamic coefficients *K(λ,0)* and *G(λ,0)* are given by Bungay and Brenner [4, 6]. These expressions are composites of asymptotic centerline results for small and for closely fitting spheres, are valid for $0 \le \lambda < 1$ and are accurate to within 10% for all values of λ (6,7). Notice that in the absence of electrostatic interactions, which is the case accounted in this study, *E*=0 and Eqs 10-11 are written as $H = \phi K^{-1}(\lambda,0)$ and $W = \phi\left(2-\phi\right)G(\lambda,0)$, where ϕ is the partition coefficient: $\phi = \left(1-\lambda\right)^2$).

Interstitial transport:

Single Stage (chemotherapy)

The equation system employed for the interstitial transport of the drug, its binding to cancer cells and its internalization by the cells is the following:

Free drug:

$$\frac{\partial C_F}{\partial t} = -v\nabla C_F + D_F\nabla^2 C_F - \frac{1}{\varphi}K_{ON}C_{rec}C_F + K_{OFF}C_B + \Phi \tag{12}$$

Bound drug:

$$\frac{\partial C_B}{\partial t} = \frac{1}{\varphi}K_{ON}C_{rec}C_F - K_{OFF}C_B - K_{INT}C_B \tag{13}$$

Internalized drug:

$$\frac{\partial C_I}{\partial t} = K_{INT}C_B \tag{14}$$

where, C_f, C_b and C_i are the concentrations of the free, bound and internalized drug in the interstitial space, C_{rec} is the concentration of cell surface receptors, v is the interstitial fluid velocity given by Darcy's law, D is the diffusion coefficient, K_{on}, K_{off} and K_{int} are the association (binding), dissociation and internalization rate constants, respectively and φ is the volume fraction of tumor accessible to the drug and Φ is the transvascular flux of the drug given by Starling's approximation.

Two Stage System (nanocarrier + drug)

The primary nano-carrier is delivered to the tumor and releases the drug. In the equations below C_N is the concentration of the carrier, K_{el} the rate constant of release of the drug from the carrier and D_N the diffusion coefficient of the carrier. We assumed the nano-carrier to contain α particles of chemotherapy. As we discuss in the main text, the choice of α does not affect our calculations because we assume the same dose of chemotherapy to be delivered independently of the load capacity of the carrier.

$$\frac{\partial C_N}{\partial t} = -v\nabla C_N + D_N\nabla^2 C_N - K_{el}C_N + \Phi \quad (15)$$

$$\frac{\partial C_F}{\partial t} = \alpha K_{el}C_N - v\nabla C_F + D_F\nabla^2 C_F - \frac{1}{\varphi}K_{ON}C_{rec}C_F + K_{OFF}C_B \quad (16)$$

$$\frac{\partial C_B}{\partial t} = \frac{1}{\varphi}K_{ON}C_{rec}C_F - K_{OFF}C_B - K_{INT}C_B \quad (17)$$

$$\frac{\partial C_I}{\partial t} = K_{INT}C_B \quad (18)$$

Multi-stage System:

C_{N1} is the concentration of the primary nanoparticle and C_{N2} is the concentration of the secondary particle. K_{el1} is the rate constant for the release of the secondary particle from the primary and K_{el2} the rate constant for the release of the drug from the secondary particle. α is the number of secondary particles released by the primary and β the number of the drug particles released by the secondary particle.

$$\frac{\partial C_{N1}}{\partial t} = -v\nabla C_{N1} + D_{N1}\nabla^2 C_{N1} - K_{el1}C_{N1} + \Phi \quad (19)$$

$$\frac{\partial C_{N2}}{\partial t} = \alpha K_{el1}C_{N1} - v\nabla C_{N2} + D_{N2}\nabla^2 C_{N2} - K_{el2}C_{N2} \quad (20)$$

$$\frac{\partial C_F}{\partial t} = \beta K_{el2}C_{N2} - v\nabla C_F + D_F\nabla^2 C_F - \frac{1}{\varphi}K_{ON}C_{rec}C_F + K_{OFF}C_B \quad (21)$$

$$\frac{\partial C_B}{\partial t} = \frac{1}{\varphi}K_{ON}C_{rec}C_F - K_{OFF}C_B - K_{INT}C_B \quad (22)$$

$$\frac{\partial C_I}{\partial t} = K_{INT}C_B \quad (23)$$

To reduce the model parameters, K_{el2} was taken to be the same as the K_{el1} and simulations were also run keeping the values of the one the same and varying the value of the other.

Fraction of killed cells

The fraction of killed cells is calculated as 1-S_F, where S_F is the fraction of surviving cells. The fraction of surviving cells is calculated from the equation: $S_F = \exp\left(-\omega \cdot I_{peak}\right)$ according to the work of Eikenberry [7]. Eikenberry fitted the

exponential decay equation to experimental data by Kerr et al. [12] for the fraction of non-small cell lung tumor cells surviving at different doses of chemotherapy (doxorubicin) in vitro. In this equation ω=0.4938 and I_{peak} is the peak intracellular concentration of chemotherapy used in [12] in ng/10^5cells. Assuming that a cell occupies $4x10^{-9}$ ml [8] and that 1 mole of doxorubicin is 579.98g, then 1 ng/10^5 cells is approximately 10^{-6} moles/L. Therefore, the fraction of surviving cells was calculated as $S_F = \exp\left(-\omega \cdot 10^6 \cdot C_I\right)$, where C_I is concentration of the internalized doxorubicin.

Boundary conditions

We modeled a bolus injection of the particles so that the concentration at the inlet of the vascular network decreases exponentially, $C_v = C_o e^{-t/K_d}$. C_o is the initial concentration at the inlet of the vascular network and K_d is a time constant that describes the exponential decay in the blood and corresponds to the blood half-life. In the case of the single stage system, C_v and K_d are the concentration and blood half-life of the chemotherapy; for the two-stage system, C_v and K_d are the corresponding values for the nano-carrier, and for the multi-stage system, C_v and K_d are the corresponding values for the primary particle. The concentration of the different delivery systems was matched so that the amount of chemotherapy to be the same in all cases. The initial amount of chemotherapy was determined as D*A in [9], where A=0.13 L^{-1} and D=100mg. Converting D*A in moles/L (using the fact that 1 mole doxorubicin is 579.98g) we get C_o=2.24x10^{-5} M chemotherapy.

In the inlet the vascular pressure is set to 30 mmHg and at the outlet is set to 5 mmHg [3, 20]. The concentrations and pressures at the boundaries of the interstitial space are set to zero as well (Supplementary Fig. S1).

Numerical Solution Strategy

The equations of the fluid transport problem are summarized below:

Poiseuille's equation	$Q = \frac{\pi D^4}{128\mu} \cdot \frac{dP}{dz}$	$\Leftrightarrow$	$Q = G_v \cdot \Delta P_v$
Starling's approximation	$Q = L_p S(P_v - P_i)$	$\Leftrightarrow$	$Q = G_w \cdot \Delta P_w$
Darcy's equation	$Q = K_t A_c \frac{\Delta P_i}{\Delta x}$	$\Leftrightarrow$	$Q = G_t \cdot \Delta P_t$

where:

$G_v = \frac{\pi D^4}{128\mu \cdot \Delta z}$ vascular conductivity

$G_w = L_p S$ transvascular conductivity

$G_t = \frac{K_t A_c}{\Delta x}$ interstitial conductivity

We first solve the steady-state fluid problem to calculate the fluid pressures. The vascular and interstitial spaces are discretized by computational nodes (Supplementary Fig. 1B). Each node belonging to the vascular space is assigned a pore diameter taken randomly by a unimodal distribution with a given mean and standard deviation. Therefore, each of the "vascular" nodes has its own values of L_p, P, and σ (Eq. 7). Conservation of fluid requires that at each node the volume of fluid entering the node is the same as the fluid exiting the node, i.e., $\sum_i Q_i = 0$ for each node *i*. This results in a linear system of equations of the form $\mathbf{G} \cdot \mathbf{P} = \mathbf{b}$, where **G** is the conductivity matrix, **P** is the vector of unknowns that contains the vascular and interstitial fluid pressures and the vector **b** of the right hand side has zero elements unless a boundary condition is applied.

Subsequently, we solve the transient transport problem to calculate the concentration of the nanoparticles and the drug. The transient nanoparticle transport problem is solved with a finite difference scheme. Central differencing for diffusion, upwind differencing for convection and an explicit Euler method for time integration were used. The connectivity between vascular and interstitial nodes remains the same as in the fluid flow problem.

One-dimensional Steady State Solution

Useful insights can be obtained from a simplified model in which the governing equations are considered under steady state conditions in a one-dimensional geometry. Here we seek the concentrations of the nanoparticles, free drug and bound drug as functions of the distance from the blood vessel wall located at x=0. A non-zero, but constant interstitial velocity is assumed that advects material away from $(v > 0)$ or toward the vessel wall $(v < 0)$. We further assume that the vascular concentration C_v varies slowly so that nearly steady state conditions develop near the blood vessel wall. The concentration of bound drug will serve as a proxy for the concentration of internalized drug which in turn determines the surviving fraction of cells. Careful organization of the resulting solutions yields analytical expressions for characteristic lengths scales that relate the penetration of each stage of the drug delivery system to the diffusion, advection, release rates and binding rates.

For the two-stage delivery system transport of the first stage is governed

$$D_{N1}\frac{d^2C_{N1}}{dx^2} - v\frac{dC_{N1}}{dx} - K_{el1}C_{N1} = 0 \qquad (24)$$

which we solve subject to the boundary conditions $C_{N1}(0) = C_v$ and C_{N1} bounded for large x where we neglect the concentration difference across the vessel. This assumption affects the magnitude of the concentration in the tissue, but does not change the penetration distances. The solution is given by

$$C_{N1}(x) = C_v \exp\left(-\frac{x}{L_{N1}}\right) \qquad (25)$$

where the characteristic length is given by $L_{N1} = \frac{2D_{N1}}{(v^2+4K_{el1}D_{N1})^{1/2}-v}$ which reduces to $L_{N1} = \left(\frac{D_{N1}}{K_{el1}}\right)^{1/2}$ in the absence of advection. We note that advection out of the vessel $(v > 0)$ increases the penetration of the first stage while advection toward the vessel $(v < 0)$ decreases penetration. After release from the primary nanoparticle transport of the free drug is governed by

$$D_F \frac{d^2C_F}{dx^2} - v\frac{dC_F}{dx} - \frac{1}{\varphi}K_{on}C_{rec}C_F + \alpha K_{el1}C_{N1} = 0 \quad (26)$$

where we have assumed that return from the bound state is much slower than the binding rate. Further we define $K_F \equiv \frac{1}{\varphi}K_{on}C_{rec}$. We solve subject to $C_{N2}(0) = 0$ and C_{N2} bounded for large x, that is, the concentration at the vessel wall is held low by rapid clearance by the blood. The concentration of the first stage is known from equation 25. We obtain

$$C_F(x) = A_F\left[\exp\left(-\frac{x}{L_F}\right) - \exp\left(-\frac{x}{L_{N1}}\right)\right] \quad (27)$$

where the characteristic length scale is given by $L_F = \frac{2D_F}{(v^2+4K_FD_F)^{1/2}-v}$ which reduces to $L_F = \left(\frac{D_F}{K_F}\right)^{1/2}$ in the absence of advection and multiplicative coefficient is $A_F = \frac{\alpha K_{el1}C_v}{D_F\left(\frac{1}{L_{N1}}\right)^2+\frac{v}{L_{N1}}-K_F}$ which reduces to $A_F = \frac{\alpha\frac{K_{el1}}{K_F}C_v}{\left(\frac{L_F}{L_{N1}}\right)^2-1}$ in the absence of advection.

In steady state the bound drug concentration may be estimated from

$$C_B = \frac{K_{on}C_{rec}}{\varphi(K_{off}+K_{int})}C_F \quad (28)$$

Analysis of multistage delivery follows a similar pattern. Equations 24 and 25 apply to the first stage as before. Transport of the second stage (secondary nanoparticle) is governed by

$$D_{N2}\frac{d^2C_{N2}}{dx^2} - v\frac{dC_{N2}}{dx} - K_{el2}C_{N2} + \alpha K_{el1}C_{N1} = 0 \quad (29)$$

which we solve subject conditions similar to those for the free drug in the two-stage system $C_{N2}(0) = 0$ and C_{N2} bounded for large x. The expression for the concentration for the second stage nanoparticle is formally similar to that for the free drug above, that is

$$C_{N2}(x) = A_2\left[\exp\left(-\frac{x}{L_{N2}}\right) - \exp\left(-\frac{x}{L_{N1}}\right)\right] \quad (30)$$

where $L_{N2} = \frac{2D_{N2}}{(v^2+4K_{el2}D_{N2})^{1/2}-v}$ and $A_2 = \frac{\alpha K_{el1} C_v}{D_{N2}\left(\frac{1}{L_{N1}}\right)^2 + \frac{v}{L_{N1}} - K_{el2}}$ which for no advection reduce to $L_{N2} = \left(\frac{D_{N2}}{K_{el2}}\right)^{1/2}$ and $A_2 = \frac{\alpha \frac{K_{el1}}{K_{el2}} C_v}{\left(\frac{L_{N2}}{L_{N1}}\right)^2 - 1}$, respectively. Now we add a third stage which is the transport of the free drug after release from the secondary nanoparticle governed by

$$D_F \frac{d^2 C_F}{dx^2} - v \frac{dC_F}{dx} - \frac{1}{\varphi} K_{on} C_{rec} C_F + \beta K_{el2} C_{N2} = 0 \qquad (31)$$

For the distribution of the free drug we obtain

$$C_F(x) = -(A_{F1} + A_{F2}) \exp\left(-\frac{x}{L_F}\right) + A_{F1} \exp\left(-\frac{x}{L_{N1}}\right) + A_{F2} \exp\left(-\frac{x}{L_{N2}}\right) \qquad (32)$$

where $L_F = \frac{2D_F}{(v^2+4K_F D_F)^{1/2}-v}$, $A_{F1} = \frac{\beta K_{el2} A_2}{D_F\left(\frac{1}{L_{N1}}\right)^2 + \frac{v}{L_{N1}} - K_F}$ and $A_{F2} = \frac{-\beta K_{el2} A_2}{D_F\left(\frac{1}{L_{N2}}\right)^2 + \frac{v}{L_{N2}} - K_F}$ which reduces to $A_{F1} = \frac{\beta \frac{K_{el2}}{K_F} A_2}{\left(\frac{L_F}{L_{N1}}\right)^2 - 1}$ and $A_{F2} = \frac{\beta \frac{K_{el2}}{K_F} A_2}{1 - \left(\frac{L_F}{L_{N2}}\right)^2}$ without advection.

Supplementary Tables and Figures

Supplementary Table 1. Values of model parameters employed in our analysis.

Parameter	**Value**	**Reference**
K_d (blood circulation decay constant)	22 h for 20 nm particles 10 h for 100 nm particles	[15, 17]
K_{el} (release rate constant)	$1.18 \times 10^{-4}\ s^{-1}$ from data of Gelatin 100 nm multistage particles $1.5 \times 10^{-5}\ s^{-1}$ fitting a first order kinetic to BIND-014 $2.1 \times 10^{-6}\ s^{-1}$ fitting a first order kinetic to Doxil	[11, 22]
K_{on} (binding rate constant)	$1 \times 10^{1} - 1 \times 10^{6}\ M^{-1}\ s^{-1}$	[19, 21]
K_{off} (unbinding rate constant)	$8 \times 10^{-3}\ s^{-1}$	[21]
K_{int} (cell uptake rate constant)	$5 \times 10^{-5}\ s^{-1}$	[21]
Vessel wall pore diameter	200 ± 60 nm (hyper-permeable tumor)	[5]
D (particle diffusion coefficient)	$5 \times 10^{-10}\ cm^2/s$ for 100 nm particles $7 \times 10^{-8}\ cm^2/s$ for 20 nm particles $3 \times 10^{-7}\ cm^2/s$ for 10 nm particles $8 \times 10^{-7}\ cm^2/s$ for 5 nm particles $3 \times 10^{-6}\ cm^2/s$ for 1 nm particles	[16]
α, β (number of particles in the nanoparticle carrier)	α=800, β=10 for a multistage 100 nm particle α=4, β=5 for a multistage 20 nm particle α=10000 for a two-stage 100 nm particle α=20 for a two-stage 20 nm particle	[14, 22]
φ (tumor volume fraction accessible to drugs)	0.3 for 1 nm particles 0.1 for 5 nm particles 0.05 for 100 nm particles	[19, 21]
C_{rec} (concentration of	$1 \times 10^{-5}\ M$	[13]

cell surface receptors)		
R (length of the domain)	0.5 cm	[3]
K_t (interstitial space hydraulic conductivity)	$3x10^{-8}$ cm^2/mmHg s	[3]
P_v (pressure at the inlet)	30 mmHg	[3]
S_v (vascular density)	200 cm^{-1}	[3]
μ_{blood} (blood viscosity)	$3x10^{-5}$ mmHg s	[2]
d (vessel diameter)	15 μm	[2]

Supplementary Figure 1. A) Computational domain showing the vascular percolation network (red color) and the boundary conditions. **B**) The domain is discretized in vascular and interstitial nodes, which are interconnected. Q_v, Q_w and Q_t denote vascular, transvascular and interstitial fluid flow rate, respectively.

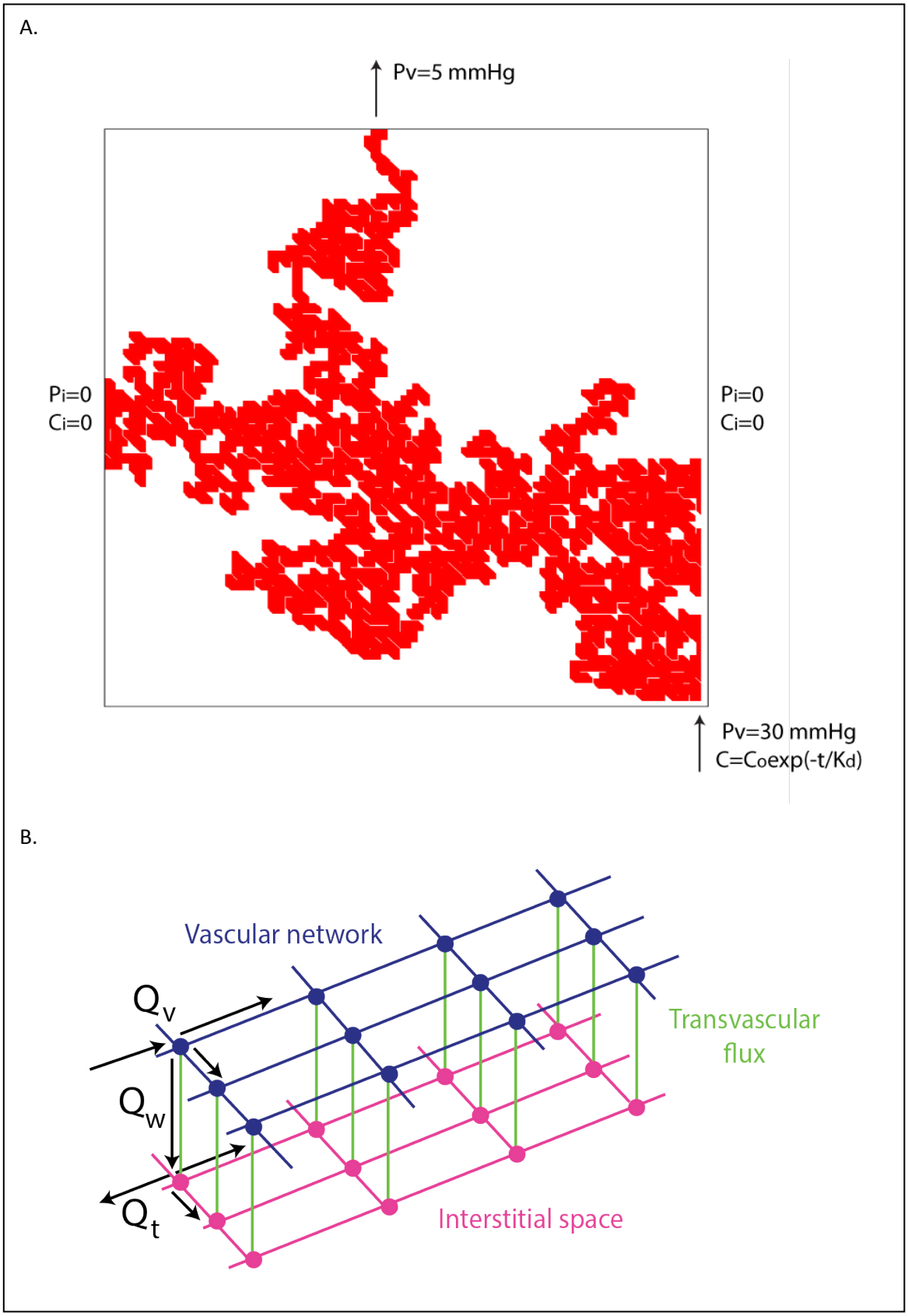

Supplementary Figure 2. Results from simplified 1-dimensional model. Optimization contour plots of the fraction of killed cells ($C_B > 0.05C_v$) as a function of binding rate constant (K_{on}) and rate constant of release (K_{el}) for the 20 nm two-stage (A) and multi-stage (B) nanoparticles neglecting advection. The maximum distance from a blood vessel is 0.05 cm. Compare to Figure 5 in the main paper.

A Two-Stage Delivery System

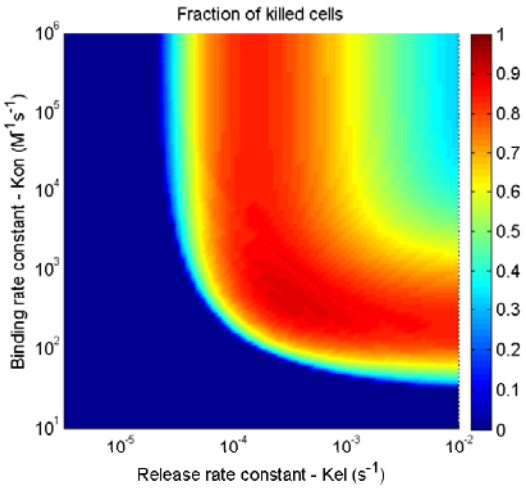

B Multi-Stage Delivery System

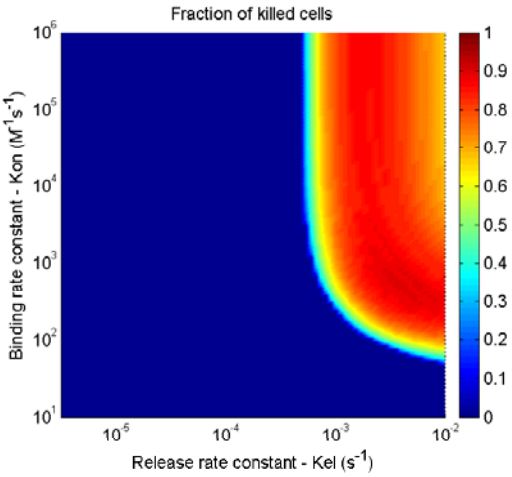

Supplementary Figure 3. Comparison of steady state multi-stage drug distribution without and with advection. Properties for a 20 nm first stage, a 5 nm second stage and a 1 nm free drug with $K_{el1} = K_{el2} = 3x10^{-3}\ s^{-1}$ and $K_{on} = 1x10^{3} M^{-1}\ s^{-1}$. No advection (A), $v = 0$ gives L_{N1}= 0.0048 cm, L_{N2}=0.0163 cm and L_F= 0.0095 cm, while flow from the vessel (B), $v = 1x10^{-5}$ cm/s gives L_{N1}=0.0068 cm, L_{N2}= 0.0181 cm and L_F =0.0096 cm. Advection by the interstitial fluid ($v > 0$) can aid distribution of the drug.

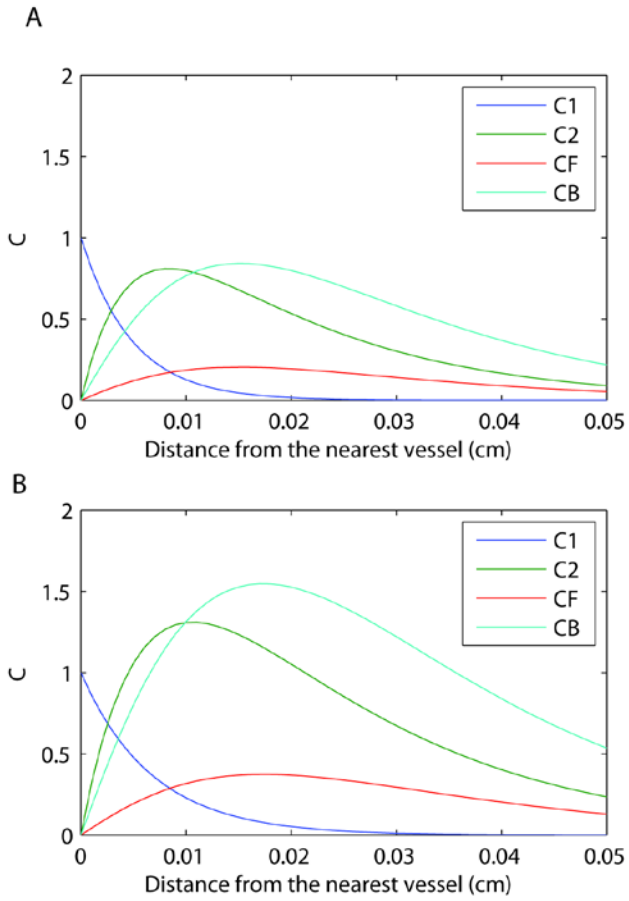

Supplementary Figure 4. Optimization contour plots for a 20 nm, two-stage nanoparticle with the ability to bind to cancer cells. Two binding rate constants of the nanoparticle were used, (A) one for low binding affinity: $1x10^2$ $M^{-1}s^{-1}$ and (B) one for high binding affinity $1x10^4$ $M^{-1}s^{-1}$. The contour plots are a function of the binding rate constant of the chemotherapy and the release rate constant from the nanoparticle. The blood half-life of the nanoparticle was taken to be K_d=10h.

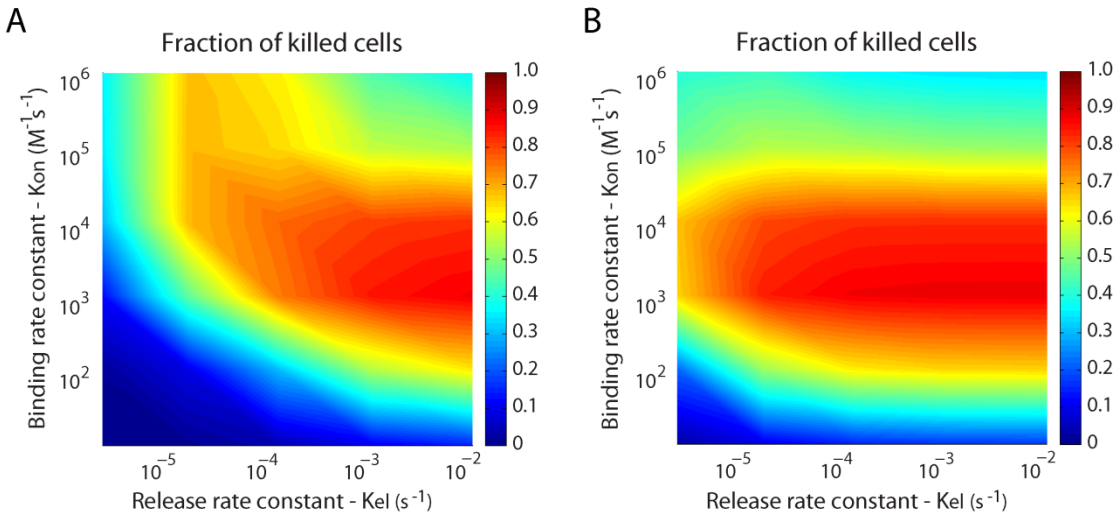

Supplementary Figure 5. Fraction of killed cells for an 100nm, multistage nanoparticle. In panel (A) the release rate constant K_{el1} of the secondary particle was kept to $1.18x10^{-4}$ s^{-1} and the release rate constant K_{el2} was varied. In panel (B) the release rate constant K_{el2} was kept to $1.18x10^{-4}$ s^{-1} and K_{el1} was varied. K_{on} was set to $1.5x10^{4}$ $M^{-1}s^{-1}$ for both cases.

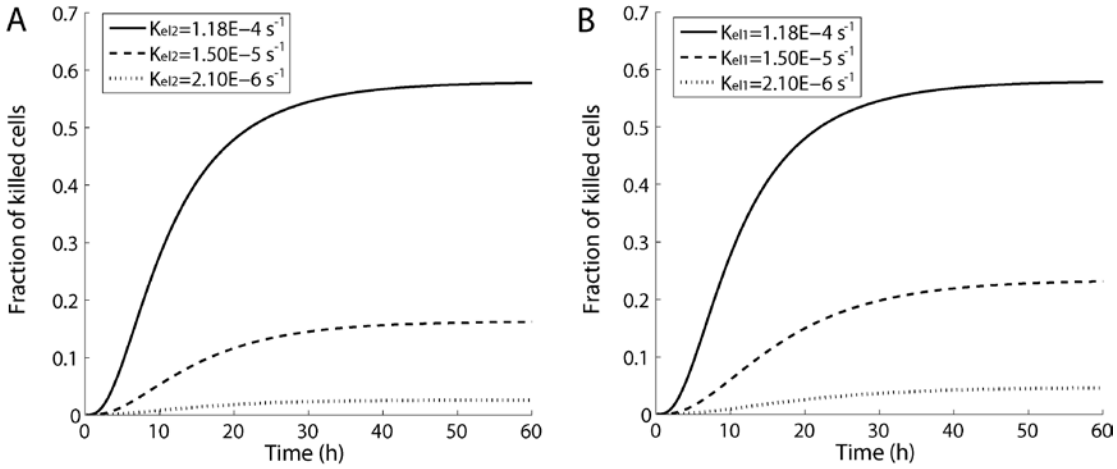

References

1. Baish, J. W., Y. Gazit, D. A. Berk, M. Nozue, L. T. Baxter, and R. K. Jain. Role of tumor vascular architecture in nutrient and drug delivery: an invasion percolation-based network model. Microvasc Res 51:327-46, 1996.

2. Baish, J. W., P. A. Netti, and R. K. Jain. Transmural coupling of fluid flow in microcirculatory network and interstitium in tumors. Microvasc Res 53:128-41, 1997.

3. Baxter, L. T. and R. K. Jain. Transport of fluid and macromolecules in tumors. I. Role of interstitial pressure and convection. Microvasc Res 37:77-104, 1989.

4. Bungay, P. M. and H. Brenner. The motion of a closely fitting sphere in a fluid-filled tube. Int. J. Multiph. Flow 1:25-56, 1973.

5. Chauhan, V. P., T. Stylianopoulos, J. D. Martin, Z. Popovic, O. Chen, W. S. Kamoun, M. G. Bawendi, D. Fukumura, and R. K. Jain. Normalization of tumour blood vessels improves the delivery of nanomedicines in a size-dependent manner. Nat Nanotechnol 7:383-388, 2012.

6. Deen, W. M. Hindered Transport of Large molecules in Liquid-Filled Pores. AIChE J 33:1409-1425, 1987.

7. Eikenberry, S. A tumor cord model for doxorubicin delivery and dose optimization in solid tumors. Theor. Biol. Med. Model. 6:16-4682-6-16, 2009.

8. El-Kareh, A. W. and T. W. Secomb. Two-mechanism peak concentration model for cellular pharmacodynamics of Doxorubicin. Neoplasia 7:705-713, 2005.

9. El-Kareh, A. W. and T. W. Secomb. A mathematical model for comparison of bolus injection, continuous infusion, and liposomal delivery of doxorubicin to tumor cells. Neoplasia 2:325-338, 2000.

10. Gazit, Y., J. W. Baish, N. Safabakhsh, M. Leunig, L. T. Baxter, and R. K. Jain. Fractal characteristics of tumor vascular architecture during tumor growth and regression. Microcirculation 4:395-402, 1997.

11. Hrkach, J., D. Von Hoff, M. Mukkaram Ali, E. Andrianova, J. Auer, T. Campbell, D. De Witt, M. Figa, M. Figueiredo, A. Horhota, S. Low, K. McDonnell, E. Peeke, B. Retnarajan, A. Sabnis, E. Schnipper, J. J. Song, Y. H. Song, J. Summa, D. Tompsett, G. Troiano, T. Van Geen Hoven, J. Wright, P. LoRusso, P. W. Kantoff, N. H. Bander, C. Sweeney, O. C. Farokhzad, R. Langer, and S. Zale. Preclinical development and clinical translation of a PSMA-targeted docetaxel nanoparticle with a differentiated pharmacological profile. Sci. Transl. Med. 4:128ra39, 2012.

12. Kerr, D. J., A. M. Kerr, R. I. Freshney, and S. B. Kaye. Comparative intracellular uptake of adriamycin and 4'-deoxydoxorubicin by non-small cell lung tumor cells in culture and its relationship to cell survival. Biochem. Pharmacol. 35:2817-2823, 1986.

13. Mok, W., T. Stylianopoulos, Y. Boucher, and R. K. Jain. Mathematical modeling of herpes simplex virus distribution in solid tumors: implications for cancer gene therapy. Clin Cancer Res 15:2352-60, 2009.

14. O'Brien, M. E., N. Wigler, M. Inbar, R. Rosso, E. Grischke, A. Santoro, R. Catane, D. G. Kieback, P. Tomczak, S. P. Ackland, F. Orlandi, L. Mellars, L. Alland, and C. Tendler. Reduced cardiotoxicity and comparable efficacy in a phase III trial of pegylated liposomal doxorubicin HCl (CAELYX/Doxil) versus conventional

doxorubicin for first-line treatment of metastatic breast cancer. Ann Oncol 15:440-9, 2004.

15. Perrault, S. D., C. Walkey, T. Jennings, H. C. Fischer, and W. C. Chan. Mediating tumor targeting efficiency of nanoparticles through design. Nano Lett. 9:1909-1915, 2009.

16. Pluen, A., Y. Boucher, S. Ramanujan, T. D. McKee, T. Gohongi, E. di Tomaso, E. B. Brown, Y. Izumi, R. B. Campbell, D. A. Berk, and R. K. Jain. Role of tumor-host interactions in interstitial diffusion of macromolecules: cranial vs. subcutaneous tumors. Proc Natl Acad Sci U S A 98:4628-33, 2001.

17. Popovic, Z., W. Liu, V. P. Chauhan, J. Lee, C. Wong, A. B. Greytak, N. Insin, D. G. Nocera, D. Fukumura, R. K. Jain, and M. G. Bawendi. A nanoparticle size series for in vivo fluorescence imaging. Angew Chem Int Ed Engl 49:8649-52, 2010.

18. Pozrikidis, C. and D. A. Farrow. A model of fluid flow in solid tumors. Ann Biomed Eng 31:181-94, 2003.

19. Schmidt, M. M. and K. D. Wittrup. A modeling analysis of the effects of molecular size and binding affinity on tumor targeting. Mol. Cancer. Ther. 8:2861-2871, 2009.

20. Stylianopoulos, T., K. Soteriou, D. Fukumura, and R. K. Jain. Cationic nanoparticles have superior transvascular flux into solid tumors: Insights from a mathematical model. Ann Biomed Eng 41(1):68-77, 2013.

21. Stylianopoulos, T. and R. K. Jain. Combining two strategies to improve perfusion and drug delivery in solid tumors. Proc Natl Acad Sci U S A 110:18632-18637, 2013.

22. Wong, C., T. Stylianopoulos, J. Cui, J. Martin, V. P. Chauhan, W. Jiang, Z. Popovic, R. K. Jain, M. G. Bawendi, and D. Fukumura. Multistage nanoparticle delivery system for deep penetration into tumor tissue. Proc Natl Acad Sci U S A 108:2426-31, 2011.